Single nucleus transcriptomics supports a role for CCNA2-induced human adult cardiomyocyte cytokinesis

Esmaa Bouhamida[1], Sangeetha Vadakke-Madathil[1#], Prabhu Mathiyalagan[4#], Amaresh K. Ranjan[1,2#], Cherrie D. Sherman[1#], Paul E Miller[3], Andre Ghetti[3], Najah Abi-Gerges[3] and Hina W. Chaudhry[1*]

[1] Icahn School of Medicine at Mount Sinai, New York, NY 10029, USA
[2] Chicago College of Pharmacy, Midwestern University, Downers Grove, IL, USA 60515
[3] AnaBios Corporation, San Diego, CA 92109, USA
[4] Benthos Prime Central, TX, USA

* Correspondence to:

Hina W. Chaudhry, M.D., Cardiovascular Regenerative Medicine, Mount Sinai School of Medicine, One Gustave L. Levy Place, Box 1030, New York, NY 10029, Phone: 212-241-4104, Fax: 212-241-5510. hina.chaudhry@mssm.edu.

Abstract

Cyclin A2 (CCNA2) is a master regulatory gene of the cell cycle that is normally silenced in postnatal mammalian cardiomyocytes. We have previously demonstrated that it can induce significant cardiac repair in both small and large animals when delivered to the heart via a viral vector. To date, whether CCNA2 gene delivery can induce cytokinesis in isolated cardiomyocytes from adult human hearts has not been investigated. Therefore, we designed a human gene therapy vector featuring a replication-deficient, E1/E3-deleted human adenovirus 5 encoding human CCNA2 driven by the cardiac Troponin T promoter to enable expression of CCNA2 in freshly isolated human cardiomyocytes. Utilizing time-lapse microscopic live imaging of cultured adult human cardiomyocytes isolated from a 21-year-old male, 41-year-old female, and 55-year-old male, we now report that human adult cardiomyocytes can be induced to undergo complete cytokinesis in response to CCNA2 gene delivery with preservation of sarcomere integrity in the resultant daughter cells. To elucidate the mechanistic underpinnings of CCNA2-dependent gene regulation in governing cardiomyocyte cytokinesis, we conducted single nucleus transcriptomics (snRNA-seq, 10X Genomics) analysis in hearts isolated from adult transgenic mice that constitutively express CCNA2 in cardiomyocytes (CCNA2-Tg) and non-transgenic mice (NTg). Remarkably, we identified a subpopulation of cardiomyocytes enriched with cytokinesis, proliferative, and reprogramming genes in hearts obtained from CCNA2-Tg mice as compared to hearts obtained from NTg mice. We also performed bulk RNA sequencing of human adult and fetal hearts, and we identified key reprogramming genes that are targets for CCNA2-induced cytokinesis. These results provide a compelling pathway forward for the clinical development of cardiac regenerative therapy based on strategic manipulation of the cardiomyocyte cell cycle.

Keywords: CCNA2; cytokinesis; single-nucleus RNA-Seq; cell cycle; heart regeneration

Introduction

The vast morbidity and mortality of heart disease is, in large part, attributed to the inability of adult human cardiomyocytes to divide in a clinically sufficient manner [1]. Scar formation via fibrosis is, therefore, the primary response to cardiac injury. A multitude of molecular and cellular approaches have been investigated over the past 20 years aimed at regenerating the myocardium in various states of heart disease [2-5]. Studies centered on the use of stem cells have remained controversial given the marginal results noted in clinical trials of cardiovascular cell therapy, and there has not been conclusive evidence of actual cardiomyocyte differentiation arising from the

cell types used in these trials. Human embryonic stem (ES) cells and induced pluripotent (iPS) cells have been evaluated in non-human primate models of heart disease with the demonstrated ability of these cell types to differentiate, at the very least, to immature cardiomyocytes with the hope that they would undergo maturation *in vivo.* However, it remains to be seen whether these approaches may be translated for human therapy [5, 6]. Aside from the differentiation and generation of new cardiomyocytes, some technical concerns still need to be addressed, such as the propensity for arrhythmias noted in primate hearts treated with ES-derived and iPS-derived cardiomyocytes[6, 7].

There has been evidence of a low level of cardiomyocyte turnover in the healthy human heart, but it is very limited, and this ability declines with age [8, 9]. Thus cardiac regeneration in response to injury such as myocardial infarction (MI) remains a challenging clinical problem with limited options at the doorstep of therapeutic translation. Evolution may not have favored adult mammals in this regard, but certain members of metazoan species are capable of heart regeneration, and these examples may perhaps serve to enlighten us. Urodele amphibians, such as the newt, retain a remarkable capacity to replace lost anatomical tissues through epimorphic regeneration [10]. This process relies on the local plasticity of differentiated cells near the region of injury and involves reentry to the cell cycle with loss of differentiated characteristics to generate a 'local progenitor cell' of restricted potentiality [10].

The adult zebrafish heart can regenerate up to 20% of its volume via a mechanism largely dependent on proliferation of cardiomyocytes adjacent to the area of injury [11, 12] However, zebrafish harboring a temperature-sensitive mutation in *mps1*, a gene encoding a mitotic checkpoint kinase [11], cannot regenerate the heart, and scarring and fibrosis are noted in the excised areas in a manner similar to the response of the human heart after injury[11-13]. These results imply that the loss of a single gene can avert cardiomyocyte mitosis and mitigate the normal regenerative process, thus permitting fibrosis to proceed unimpeded.

We have demonstrated that cyclin A2 is a 'master regulator' of the cardiomyocyte cell cycle [14]. Unlike other cyclins, cyclin A2 complexes with its cyclin-dependent kinase partners to mediate both of the two transitions of the cell cycle: G1-S and G2-M [15-17] and is silenced shortly after birth in mammalian cardiomyocytes [18-20]. We subsequently have shown that cyclin A2 mediates cardiac repair by inducing cardiomyocyte mitoses after MI in two small animal models of MI [21-23] . As molecular mechanisms may be widely divergent across species, we performed a therapeutic efficacy study of cyclin A2-mediated cardiac repair in a porcine model of MI as it closely mimics human anatomy and physiology [24]. Therapeutic delivery of CCNA2 one week after MI in the porcine heart induced cardiomyocyte cell cycle activation *in vivo* with marked

enhancement of cardiac function as noted with multimodality imaging, including magnetic resonance imaging. The experimental pigs also exhibited significantly decreased fibrosis, lack of cardiomyocyte hypertrophy, and a 55% increase in cardiomyocyte cell numbers in the peri-infarct zones. Using the same viral vector encoding CCNA2 that was delivered *in vivo*, cultured porcine adult cardiomyocytes were induced to undergo cytokinesis with preservation of sarcomere structure.

As a necessary prerequisite on the path to clinical translation, we designed the next-generation gene therapy vector using a cardiomyocyte-specific promoter, cardiac Troponin T (cTNT), driving human CCNA2 expression **(Suppl. Figure 1)**. We then sought to determine whether this cTNT-CCNA2 vector would induce human adult cardiomyocytes to undergo cytokinesis. We utilized live imaging microscopy after dynamically labeling the sarcomere within the adult human cardiomyocytes. We use single nucleus RNA-seq (snRNA-seq, 10x Genomics) to further investigate the molecular mechanisms of CCNA2-induced cardiomyocyte cytokinesis **(Suppl. Figure 1)**.

Methods

Ethics Statement

This study was conducted in accordance with the Declaration of Helsinki. This study used cardiomyocytes from adult human heart tissues provided by Anabios, San Diego, CA. The specimens used in this research are fully de-identified and therefore are exempt from ethics approval.

Culture of Adult Human Cardiomyocytes and *In Vitro* Cytokinesis Study

Cardiomyocytes from adult human (21-year-old male, 41-year-old female, and 55-year-old male) heart tissue were isolated after enzymatic digestion at Anabios, San Diego, CA, and were shipped to our laboratory within 24 hours of isolation. Adult human cardiomyocytes were subjected to culture similar to our previously published adult porcine cardiomyocyte culture technique [24] with slight modification. In brief, upon arrival, cells were washed with serum-free DMEM media twice, and 105 cells were seeded in 100mm untreated polystyrene plates. Non-adherent cells were collected every 24 hours and centrifuged at 20Xg for 2 min at room temperature. Cell pellet was washed with serum-free DMEM and seeded on new polystyrene plates in modified Cardiomyocyte Culture Media [24] (mod CMC) formulated by adding 13% FBS, 2.5% horse serum, 1X nonessential amino acid, 1mM sodium pyruvate, penicillin (100 U/ml), streptomycin (100 mg/ml), and fungizone (0.5 mg/ml) to Dulbecco's modified Eagle's medium (DMEM)/F12 (50:50). Cells

were washed every day with serum-free DMEM, re-seeded in new polystyrene plates and cultured for 3 days. On day 4, they were seeded in glass-bottom 24-well tissue culture plates for 20 days, with the medium changed every 4th day. The wells with cardiomyocytes exhibiting adhesion and spreading were selected. Cells in these wells were trypsinized and counted, and 10^3 cells per well were seeded in new glass bottom tissue culture plates. After 2 days of culture, cells were divided into two groups (test and control) and were transfected with adenoviruses. The test group was transfected with cTnT-hCCNA2 along with cTnT-eGFP and/or cTnT-H2B-GFP and CMV-α-actinin-mCherry adenoviruses while the control group was transfected with only cTnT-eGFP and/or cTnT-H2B-GFP and CMV-α-actinin-mCherry adenoviruses. The multiplicity of infection (MOI) of adenoviruses were adjusted to 180 in each well of test (with cTnT-hCCNA2; MOI 100, CMV-α-act-mCherry; MOI 40 and cTnT-eGFP or cTnT-H2B-GFP; MOI 40) and control (cTnT-eGFP; MOI 140 and CMV-α-act-mCherry; MOI 40) group. After 48 hours of incubation, transfection was confirmed by observing the desired fluorescence in live cell imaging with Zeiss AxioVision Observer Z1 inverted microscope (Carl Zeiss). We also tested the differentiation potential (active calcium flux and sarcomere structure) of cardiomyocytes after cytokinesis *in vitro* by culturing them in agarose-based semi-solid medium for 2 weeks. Cardiomyocytes were subjected to calcium flux imaging with pacing of 0.5 Hz and 1 Hz current. Cells were fixed in 4% paraformaldehyde, and fluorescence microscopy was carried out to detect the α-act-mCherry and sarcomere structure.

Time-lapse microscopy

To capture cell division events in cardiomyocytes *in vitro*, we carried out live cell epifluorescence time-lapse microscopy as described earlier [24]. In brief, Zeiss AxioVision Observer Z1 (Carl Zeiss, Thornwood, NY, USA) inverted epifluorescence microscope in a humidified chamber in the presence of 5% CO_2 at 37°C was used to carry out time-lapse microscopy. Multiple random points with cells expressing eGFP (green) and mCherry (red) were selected in the test and control groups. The positions were marked with the “position-list” tool in the AxioVision microscopy software (AxioVision Release 4.7, Carl Zeiss). After the first cycle of imaging, only the channel for Texas red was used (for detection of mCherry) to acquire images for 72 hours. The fluorescein isothiocyanate (green) channel of the microscope was kept closed during the time-lapse imaging to avoid cell death from exposure to ultraviolet rays in this channel. Images were taken at intervals of 30 min. The objective lens of 10X was used for all time-lapse imaging. Time-lapse movies were generated after the end of each experiment and exported as MOV files. The time-lapse movies were analyzed, and cells that underwent successful cytokinesis

were enumerated in each group. The % cytokinesis events were calculated for each position, and the graph was plotted.

Cell fixation and nuclear staining

After time-lapse microscopy, cells in the glass-bottom plate were fixed with 4% paraformaldehyde at room temperature for 20 min and were stored in 4°C. For nuclear staining, cells were washed with 1XPBS and permeabilized by incubating them in 0.5% Triton X-100 solution for 20 min at room temperature. Cells were washed three times with 1XPBS and incubated in DAPI solution (2.5 ↗g/ml) for 5 min. Cells were washed twice with 1X PBS, and imaging was carried out using a Zeiss AxioVision Observer Z1 inverted epifluorescence microscope.

Real-time quantitative PCR

Quantitative PCRs were performed in cultured cardiomyocytes transfected with cTnT-hCCNA2 (test) or cTnT-eGFP (control) adenovirus with similar MOI (MOI 100). “SYBR Green quantitative PCR protocol” on the “StepOnePlus” real-time PCR system (Applied Biosystems, CA) was used. The PCR protocol consisted of one cycle at 95°C for 2 min, 39 cycles at 95°C for 15 sec + 60°C for 1 min, and then 4°C on hold. Gene expression was determined by using the formula 2^(39-👎👎CT) with consideration of CT value 39 for a single transcript and with normalization to the endogenous control GAPDH.

Animal

Cyclin A2 transgenic mice (Jackson Laboratory, Bar Harbor, Maine) [14] adult males and females of 8-12 weeks old were maintained in a B6CBA background. Non-transgenic (wild-type) littermates were used as our controls. All manipulations were performed according to Institutional Animal Care and Use Guidelines.

Collection of CCNA2-Tg mouse hearts

Sample preparation for Single Nucleus RNA-sequencing (snRNA-seq)

Frozen heart tissues from CCNA2-Tg- and non-Tg adult mice, male and female, were minced and transferred into a Dounce homogenizer containing cold lysis buffer (Benthos Prime Central, TX, USA). Samples were homogenized gently, and nuclei were isolated. Nuclei were ensured to be free of clumps and debris by trypan blue staining under a microscope. Nuclei were then counted, and concentration was adjusted. 10x library concentration, insert size, and quantification were

checked using Qubit, Agilent bioanalyzer, and q-PCR, respectively. For data Processing and Quality Control of 10x Sequencing of snRNA-seq, the reads were processed with CellRanger software (v.3.1.0) (10x Genomics) with the default parameters for each sample separately. This involved various steps, including alignment to a reference, collapsing of unique molecular identifiers (UMIs), UMI counting, and initial quality control procedures. The outcome of this process was the generation of filtered gene expression matrices that exclusively contained cellular barcodes. Subsequently, the Seurat R package (v.3.1.1) was employed to further enhance data quality control. Cell Ranger employs the STAR aligner for splicing-aware mapping of reads to the genome. Subsequently, it utilizes a transcript annotation GTF file to categorize the reads into exonic, intronic, and intergenic regions based on whether the reads align confidently with the genome. Only confidently mapped, non-PCR duplicates with valid barcodes and UMIs were used to generate a gene-barcode matrix. The filtered_feature_bc_matrix generated by Cell Ranger was used for Seurat processing. Cell marker identification was carried out using the cell-specific markers dataset provided at iRhythmics FairdomHub instance under https://fairdomhub.org/studies/739.

Human Fetal and Adult Hearts and RNA sequencing

Human fetal heart RNA (n=3 pooled, Cat #636532, Takara) and human adult heart RNA (n=4 pooled, Cat #636583, Takara) were used for bulk RNA sequencing. Briefly, total RNA was used for rRNA depletion, followed by directional library preparation and sequencing. The sequence reads were mapped to the human genome (GRCh38.110) using STAR [25] (version 2.7.9a). Using the mapped reads, the R package edgeR [26] (version 3.30.3) was employed to calculate counts per million (CPM) values and false discovery rate (FDR)-adjusted p-values obtained through the Benjamini–Hochberg method (Benthos Prime Central, TX, USA).

Data availability

The processed single-cell data and the bulk RNA sequencing, including raw expression matrices and raw sequence files that support the findings of this research study, are available on the Gene Expression Omnibus GSE249433 and GSE256519, respectively.

Statistical analysis

All data generated in this study were analyzed with an unpaired t-test. Data are presented as means ± SEM unless otherwise indicated. Significance was considered to be $P < 0.05$.

Results

cTnT-CCNA2 adenovirus vector designed for therapeutic use induces expression of CCNA2 in cultured adult human cardiomyocytes. The therapeutic use grade human CCNA2 adenovirus vector was designed to express human cyclin A2 (CCNA2) specifically in cardiomyocytes by cloning human cDNA (NCBI Reference Sequence: NM_001237.4; 374-1672 bp) downstream to the cardiac Troponin T (cTnT) promoter **(Figure 2A)**. The cultured adult human cardiomyocytes were transfected with cTnT-hCCNA2 (test) and cTnT-eGFP and/or cTnT-H2B-GFP (control) adenoviruses with MOI of 100 each for assessing the induced expression of CCNA2. We observed significantly increased expression of CCNA2 in the cultured adult human cardiomyocytes transfected with the test compared to the control adenovirus (**Figure 2B**).

Adenoviral vector-mediated expression of CCNA2 induces cytokinesis in cultured adult human cardiomyocytes.

To assess the effect of induced CCNA2 expression on cell division in adult human cardiomyocytes, we cultured adult human cardiomyocytes and studied cytokinesis *in vitro* by using live cell epifluorescence time-lapse microscopy. The adult human cardiomyocytes were plated at equal densities and transfected with cTnT-hCCNA2, cTnT-eGFP and/or cTnT-H2B-GFP and CMV-α-act-mCherry adenoviruses (test) or with cTnT-eGFP and/or cTnT-H2B-GFP and CMV-α-act-mCherry adenoviruses (control). cTnT-eGFP and/or cTnT-H2B-GFP adenovirus was transfected in both groups to confirm the initial tracking of cardiomyocytes (green) during live cell epifluorescence microscopy. For delineation of sarcomeric structure in cardiomyocytes, cells from both groups were co-transfected with adenovirus containing α-actinin-mCherry, which was constructed to allow for proper folding of the virally delivered α-actinin into the live cardiomyocyte sarcomere (CMV-α-act-mCherry) and was successfully used in cultured adult porcine cardiomyocytes [24]. This strategy enables us to confirm cardiomyocyte identity by assessing the expression of eGFP before and after cytokinesis and tracking of sarcomere dynamics during live cell imaging. This strategy is more accurate than antibody-based identification which can result in artifact and can only be used at one time point after cell fixation. We observed co-expression of eGFP (green) and α-actinin (red) in cultured adult cardiomyocytes **(Figure 2A** and **2E**; first panel). We performed time-lapse microscopic imaging of live cells to capture cardiomyocyte cytokinesis **(Figure 2A** and **2E**; still images from **movie S1)**. We calculated the cytokinetic index of adult human cardiomyocytes by counting cytokinetic events observed in 42 regions of interest (ROIs) **(table S1)**. The cytokinetic index was significantly higher in the test samples with cTnT-CCNA2 adenovirus transfection compared to control samples in the 41- and 55-year-olds **(Figure 2F)**. In

contrast, no significant change in the cytokinetic events between test and control samples was observed in the 21yo patient's cardiomyocytes **(Figure 2F)**. Most remarkably, sarcomere structure was preserved in the daughter cells after cytokinesis **(Figure 2B**; upon magnification of a daughter cell, the presence of sarcomeric structure is easily noted). The daughter cells were further identified with the expression of eGFP and/or H2B-GFP (as they were originally also transfected with cTnT-eGFP and/or H2B-GFP) and noted to be mononuclear after they had been fixed and stained with DAPI **(Figure 2C** and **2E)**. Clusters of other cardiomyocytes with expression of eGFP that had not taken up the Ad5-α-act-mCherry could be seen adjacent to the daughter cells **(Figure 2C)**. To confirm cardiomyocyte differentiation and preservation of sarcomeric structure in both parent and daughter cells, we measured differentiation potential by subjecting the cardiomyocytes to calcium flux imaging with pacing of 0.5 Hz and 1 Hz current and detected α-act-mCherry and sarcomere structure by fluorescence microscopy, respectively **(Figure 3A)**. We observed that 4-5% of Ad5-cTnT-hCCNA2 transfected adult human cardiomyocytes show active Ca++ mobilization **(Figure 3B)**. Subsequently, these cardiomyocytes were fixed with 4% paraformaldehyde, and fluorescence microscopy was carried out to detect α-act-mCherry. A representative magnified fluorescence micrograph of adult human cardiomyocyte post-differentiation clearly shows a very distinct sarcomere structure **(Figure 3C)**.

Single nucleus transcriptomic (snRNA-seq) analysis of CCNA2-Tg mouse hearts identifies CCNA2-induced reprogramming genes in a selective subset of cardiomyocytes.

To explore the full spectrum of CCNA2-induced cardiomyocyte cytokinesis in an unbiased manner, we performed snRNA-seq on adult hearts isolated from control non-transgenic (non-Tg) and CCNA2 constitutively expressing transgenic mice (CCNA2-Tg). We included both male and female mice at 8-12 weeks old for our study **(Figure 4A** and **4B)**. This extensive dataset allows the identification of critical differentially expressed genes in cellular clusters throughout the heart of both non-Tg and CCNA2-Tg mice, in which CCNA2 is highly increased**.**

Data visualization using a tSNE plot shows more than 14 distinct cell types in both non-Tg and CCNA2-Tg mice and identified several common clusters between non-Tg and CCNA2-Tg mice, of which mature cardiomyocytes, neuronal cell population, and others **(Figure 4C)**. Cardiomyocyte populations were identified by classical marker genes (*Actn2,* and *Tnnc1)* in both non-Tg and CCNA2-Tg hearts*.* Cardiomyocytes that express an enhanced level of markers of contractility, including the *Ryr2,* are designated as mature cardiomyocytes [27]. However, in CCNA2-Tg mouse hearts, we identified two distinct subclusters within the cardiomyocyte

population **(Figure 4C)**. These two distinct subclusters are exclusive to the cardiomyocyte population present in CCNA2-Tg mouse hearts as compared to non-Tg mouse hearts. Examining the transcriptome of these two distinct cardiomyocyte subclusters in CCNA2-Tg hearts, we identified one subcluster showing specific expressions of cardiomyocyte immature markers such as *Myh7*, *Rrad,* and expressing low levels of *Ryr2,* which we labeled “immature cardiomyocytes”, while the other subcluster showed expressions of proliferative cardiomyocyte markers such as *Actc1, Mki67, and Kif23*, which we labeled “proliferative cardiomyocytes” **(Figure 4C).** CCNA2 expression was confirmed in cardiomyoctes including subsets of cardiomyocytes identified in CCNA2-Tg mice (**Figure 5**). A global comparison of immature and proliferative gene expression across all cardiomyocytes reveals that these genes are specifically expressed in CCNA2-Tg mice compared to non-Tg mice **(Figure 6B)**.

To understand CCNA2-induced cytokinesis events, we asked whether these unique subclusters of cardiomyocytes in CCNA2-Tg mice show expression of genes involved in cytokinesis and/or reprogramming. Interestingly, both “immature cardiomyocytes” and” ventricular proliferative cardiomyocytes” clusters showed specific expressions of cytokinesis (*Aurkb*, *Anln*, *Sept7*, *Rho,* and others) and reprogramming genes *(Klf4, Gata4, Myc, Sox2),* as compared to the mature cardiomyocytes cluster in CCNA2-Tg and non-Tg **(Figure 6C)**

It is noteworthy to mention that in the adult murine context, approximately 85–90% of cardiomyocytes exist in a binucleated state [28], indicating that the nuclear count does not precisely correspond to the cell count. Furthermore, the polyploidization of cardiomyocytes has been recognized as an impediment to heart regeneration [29]. It has been established that binucleated cardiomyocytes re-entering the cell cycle exhibit a failure to complete cytokinesis, thereby impeding the efficient regeneration of cardiac tissue following injury [30].

To investigate whether such reprogramming genes are downregulated in adult human hearts, we carried out bulk RNA-sequencing in the hearts of fetal and adult human hearts. Transcriptomic analysis of human hearts revealed that a number of cytokinesis (*Aurkb*, *Anln*, *Sept7*, *Rho,* and others) and reprogramming *(Klf4, Gata4, Myc, Sox2,* and others*)* genes induced in CCNA2-Tg mouse hearts were decreased for expression in human adult hearts as compared to fetal human hearts **(Figure 6D)**. Our study establishes a molecular mechanism by which CCNA2 induces the reprogramming genes, which ultimately enhances the cardiomyocyte cytokinesis. These results provide a compelling pathway forward for the clinical development of cardiac regenerative therapy based on the manipulation of the cardiomyocyte cell cycle.

Discussion

Epimorphic regeneration is a conserved mechanism across evolutionary biology, permitting organ-specific tissue regeneration in a variety of metazoan phylogeny, including early postnatal mammals [30]. In fact, in human neonates, the ventricular myocardium responds to the pressure overload of congenital aortic stenosis through hyperplastic growth, yet the degenerative, calcific aortic stenosis of older patients elicits hypertrophic growth of the myocardium [32-34] These clinical observations imply that the cell cycle repertoire of human neonatal cardiomyocytes is also intact, as cardiac growth is able to occur in a similar fashion to the embryonic heart. Moreover, the adult human heart is also capable of a very low rate of turnover [8], with diminishing rates of turnover past childhood and adolescence, with cardiomyocyte cytokinesis not evident past age 20 [9].

Strategies to induce cardiomyocyte cytokinesis in adult human hearts are of critical need in order to face the growing public health crisis of congestive heart failure. To our knowledge, most cell therapy clinical trials in heart disease have provided inconsistent evidence of improvements in left ventricular ejection fraction, with a lack of evidence that cell types utilized actually differentiate into functional cardiomyocytes. To this end, we previously explored the effects of cell cycle manipulation in small and large animal models and successfully induced cardiomyocyte proliferation *in vivo* with significant enhancement of cardiac function in animal models [21-24]. In any translational plan to use cell cycle regulators for clinical use, precautions must be in place to prevent the expression of cell cycle activators in extra cardiac tissues due to the potential for oncogenic transformation [35]. This safety concern prompted us to explore methods of tissue-specific activation of cyclin A2. One such method was to design a next-generation viral vector in which a cardiomyocyte-specific promoter, cardiac Troponin T, drives the expression of human cyclin A2 (cTnT-hCCNA2). Human cardiomyocytes isolated from 21-, 41- and 55-year-olds who had died of noncardiac causes were cultured utilizing adult mammalian cardiomyocyte culture methods developed by our laboratory [24] and transfected with cTnT-hCCNA2. Cardiomyocytes from the 41- and 55-year-olds in the experimental wells underwent complete cytokinesis at a significantly higher frequency than the cardiomyocytes in the control wells. Based on our previous studies of rodent cardiomyocytes, we attribute the low rate of cytokinetic events we observed in the control wells to the reactivation of endogenous CCNA2 with the prolonged culture of cardiomyocytes. This is a phenomenon we have previously observed and quantified in rodent cardiomyocytes (unpublished data), and likely not correlated with the low turnover seen in human hearts as measured by ^{14}C dating [8] as cytokinesis markers were not noted at all in human hearts over the age 20 by Kühn and colleagues [9]. Similarly, Frisén and colleagues [36] used stereological and ^{14}C quantification techniques to measure cardiomyocyte exchange. They found

that most cardiomyocytes were never exchanged and that the substantial replacement of existing cardiomyocytes were generated in the first 10 years of life, while the second decade of life focused on DNA polyploidization. Cardiomyocyte plasticity plays a key role in cardiac remodeling and repair in infarcted hearts [37]. Our snRNA-Seq also confirms heightened cardiomyocyte plasticity of Ccna2 transgenic mice as we note changes in gene expression involved in cell cycle progression and reprogramming. Calcium signaling is a fundamental pathway in the regulation of cell division, cardiac contractility, and remodeling [38, 39]. The increase in the cytokinetic index in the test samples from 41- and 55-year-olds shows the ability of CCNA2 to stimulate intracellular Ca++ mobilization. Of note, the transfected cTnT-hCCNA2 (test samples) cultured cardiomyocytes isolated from a 21-year-old male did not show a significant increase in cytokinetic index invoked by CCNA2 when compared to the control samples, which is consistent with reports of previous investigators (9, 36) that cell turnover and cell division can naturally occur at younger ages in humans.

SnRNA-seq has been used to identify transcriptomic changes occurring at the single-cell level, shedding light on precise mapping of transcriptomics alterations in a cell-type specific manner in response to cellular stimulation or gene delivery [40]. Employing snRNA-seq in intact tissues enables capturing of cell-specific transcriptomics changes in a more precise manner while maintaining the integrity of tissue responses, compared to isolated *in vitro* transcriptomics analyses. Our strategy of using snRNA-se to identify cardiomyocyte-specific changes in an *in vivo* setting in a clinically relevant Tg-CCNA2 model allowed us to map specific changes to a subpopulation of cardiomyocytes, which would not have been captured by analyzing the transcriptome of the bulk tissue of isolated cardiomyocytes using bulk RNA-seq strategies.

Furthermore, the genes induced in the Tg-CCNA2 model appear to be representing a common mechanism underlying cytokinesis in both male and female mice, consistent with observations in human male and female hearts. Given that we identified a subset of cardiomyocytes being reprogrammed into a more proliferative state, our next goal is to investigate this cardiomyocyte subset population more definitively. Once we define the transcriptomic state and its proliferative potential in greater detail, we will focus on recapitulating such proliferative cardiomyocytes both *in vitro* and *in vivo* to investigate whether targeting these specific subpopulations holds greater therapeutic potential than targeting the entire cardiomyocyte population.

Acknowledgment:

We thank Dr. Bernhard Kühn for his contribution of the cTnT-H2B-GFP utilized in this study.

Conflict of interests:

The authors report no conflict of interest. H.W.C. is the founder and equity holder of VentriNova, Inc and listed inventor on multiple patents regarding cyclin A2-mediated cardiac repair and caudal-related homeobox 2 cells for cardiac repair.

References:

1. Laflamme, M.A. and C.E. Murry, *Heart regeneration.* Nature, 2011. **473**(7347): p. 326-35.
2. Miyamoto, K., et al., *Direct In Vivo Reprogramming with Sendai Virus Vectors Improves Cardiac Function after Myocardial Infarction.* Cell Stem Cell, 2018. **22**(1): p. 91-103 e5.
3. Cuculich, P.S., et al., *Noninvasive Cardiac Radiation for Ablation of Ventricular Tachycardia.* N Engl J Med, 2017. **377**(24): p. 2325-2336.
4. Yoshida, Y. and S. Yamanaka, *Induced Pluripotent Stem Cells 10 Years Later: For Cardiac Applications.* Circ Res, 2017. **120**(12): p. 1958-1968.
5. Doppler, S.A., et al., *Mammalian Heart Regeneration: The Race to the Finish Line.* Circ Res, 2017. **120**(4): p. 630-632.
6. Shiba, Y., et al., *Allogeneic transplantation of iPS cell-derived cardiomyocytes regenerates primate hearts.* Nature, 2016. **538**(7625): p. 388-391.
7. Chong, J.J., et al., *Human embryonic-stem-cell-derived cardiomyocytes regenerate non-human primate hearts.* Nature, 2014. **510**(7504): p. 273-7.
8. Bergmann, O., et al., *Evidence for cardiomyocyte renewal in humans.* Science, 2009. **324**(5923): p. 98-102.
9. Mollova, M., et al., *Cardiomyocyte proliferation contributes to heart growth in young humans.* Proc Natl Acad Sci U S A, 2013. **110**(4): p. 1446-51.
10. Brockes, J.P. and A. Kumar, *Plasticity and reprogramming of differentiated cells in amphibian regeneration.* Nat Rev Mol Cell Biol, 2002. **3**(8): p. 566-74.
11. Poss, K.D., L.G. Wilson, and M.T. Keating, *Heart regeneration in zebrafish.* Science, 2002. **298**(5601): p. 2188-90.
12. Jopling, C., et al., *Zebrafish heart regeneration occurs by cardiomyocyte dedifferentiation and proliferation.* Nature, 2010. **464**(7288): p. 606-9.
13. Furtado, M.B., et al., *View from the heart: cardiac fibroblasts in development, scarring and regeneration.* Development, 2016. **143**(3): p. 387-97.
14. Chaudhry, H.W., et al., *Cyclin A2 mediates cardiomyocyte mitosis in the postmitotic myocardium.* J Biol Chem, 2004. **279**(34): p. 35858-66.
15. Nurse, P., *A long twentieth century of the cell cycle and beyond.* Cell, 2000. **100**(1): p. 71-8.
16. Pagano, M., et al., *Cyclin A is required at two points in the human cell cycle.* EMBO J, 1992. **11**(3): p. 961-71.
17. Sherr, C.J. and J.M. Roberts, *Inhibitors of mammalian G1 cyclin-dependent kinases.* Genes Dev, 1995. **9**(10): p. 1149-63.
18. Wang, B.J. and H.W. Chaudhry, *Regulation of Cardiomyocyte Division During Cardiac Regeneration.* Curr Cardiol Rep, 2023. **25**(7): p. 615-620.
19. Vadakke-Madathil, S. and H.W. Chaudhry, *Cardiac Regeneration: Time to Revisit Nature.* Circ Res, 2018. **123**(1): p. 24-26.
20. Yoshizumi, M., et al., *Disappearance of cyclin A correlates with permanent withdrawal of cardiomyocytes from the cell cycle in human and rat hearts.* J Clin Invest, 1995. **95**(5): p. 2275-80.
21. Cheng, R.K., et al., *Cyclin A2 induces cardiac regeneration after myocardial infarction and prevents heart failure.* Circ Res, 2007. **100**(12): p. 1741-8.

22. Woo, Y.J., et al., *Therapeutic delivery of cyclin A2 induces myocardial regeneration and enhances cardiac function in ischemic heart failure.* Circulation, 2006. **114**(1 Suppl): p. I206-13.
23. Woo, Y.J., et al., *Myocardial regeneration therapy for ischemic cardiomyopathy with cyclin A2.* J Thorac Cardiovasc Surg, 2007. **133**(4): p. 927-33.
24. Shapiro, S.D., et al., *Cyclin A2 induces cardiac regeneration after myocardial infarction through cytokinesis of adult cardiomyocytes.* Sci Transl Med, 2014. **6**(224): p. 224ra27.
25. Dobin, A., et al., *STAR: ultrafast universal RNA-seq aligner.* Bioinformatics, 2013. **29**(1): p. 15-21.
26. Robinson, M.D., D.J. McCarthy, and G.K. Smyth, *edgeR: a Bioconductor package for differential expression analysis of digital gene expression data.* Bioinformatics, 2010. **26**(1): p. 139-40.
27. Galow, A.M., Wolfien M., et al. *Integrative Cluster Analysis of Whole Hearts Reveals Proliferative Cardiomyocytes in Adult Mice*. Cells. 2020 May 6;9(5):1144.
28. Soonpaa, M.H., et al., *Cardiomyocyte DNA synthesis and binucleation during murine development.* Am J Physiol, 1996. **271**(5 Pt 2): p. H2183-9.
29. Gonzalez-Rosa, J.M., et al., *Myocardial Polyploidization Creates a Barrier to Heart Regeneration in Zebrafish.* Dev Cell, 2018. **44**(4): p. 433-446 e7.
30. Bersell, K., et al., *Neuregulin1/ErbB4 signaling induces cardiomyocyte proliferation and repair of heart injury.* Cell, 2009. **138**(2): p. 257-70.
31. Porrello, E.R., et al., *Transient regenerative potential of the neonatal mouse heart.* Science, 2011. **331**(6020): p. 1078-80.
32. Leeuwenburgh, B.P., et al., *Chronic right ventricular pressure overload results in a hyperplastic rather than a hypertrophic myocardial response.* J Anat, 2008. **212**(3): p. 286-94.
33. Assey, M.E., et al., *Unexpected persistence into adulthood of low wall stress in patients with congenital aortic stenosis: is there a fundamental difference in the hypertrophic response to a pressure overload present from birth?* Circulation, 1987. **75**(5): p. 973-9.
34. Torp, K.H., *Congenital aortic stenosis with hyperplasia of the endocardium in the left ventricle.* Acta Pathol Microbiol Scand, 1951. **29**(2): p. 109-19.
35. Wang, J., et al., *Hepatitis B virus integration in a cyclin A gene in a hepatocellular carcinoma.* Nature, 1990. **343**(6258): p. 555-7.
36. Bergmann, O., et al., *Dynamics of Cell Generation and Turnover in the Human Heart.* Cell, 2015. **161**(7): p. 1566-75.
37. Gong, R., et al., *Regulation of cardiomyocyte fate plasticity: a key strategy for cardiac regeneration.* Signal Transduct Target Ther, 2021. **6**(1): p. 31.
38. Rosendo-Pineda, M.J., C.M. Moreno, and L. Vaca, *Role of ion channels during cell division.* Cell Calcium, 2020. **91**: p. 102258.
39. Liu, C., et al., *Alteration of calcium signalling in cardiomyocyte induced by simulated microgravity and hypergravity.* Cell Prolif, 2020. **53**(3): p. e12783.
40. Bode, D., Cull, AH., Rubio-Lara, JA., Kent, DG. *Exploiting Single-Cell Tools in Gene and Cell Therapy*. Front Immunol. 2021 Jul 12;12:702636.

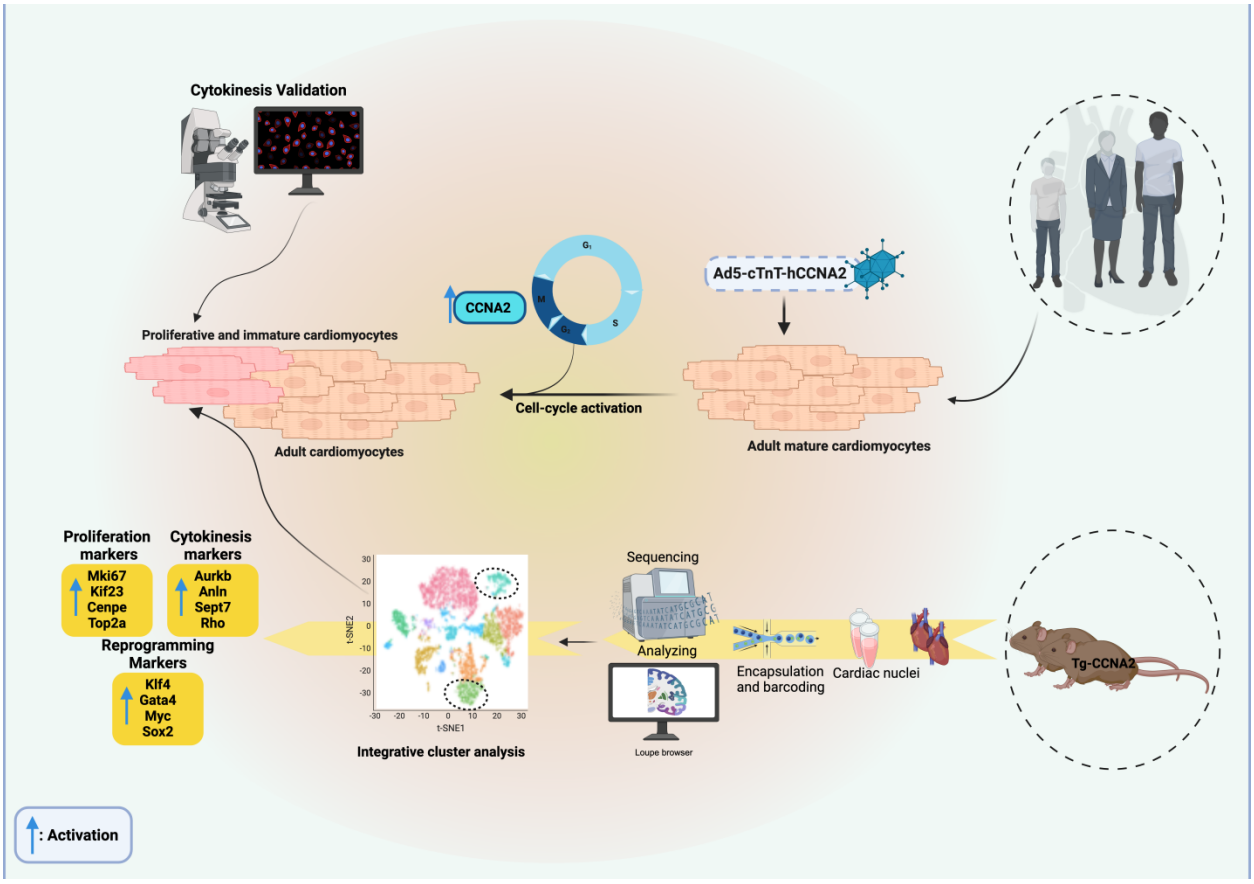

Figure 1: Constitutive expression of CCNA2 in adult cardiomyocytes elicits the induction of cytokinesis and proliferative and reprogramming genes in both humans and mice.

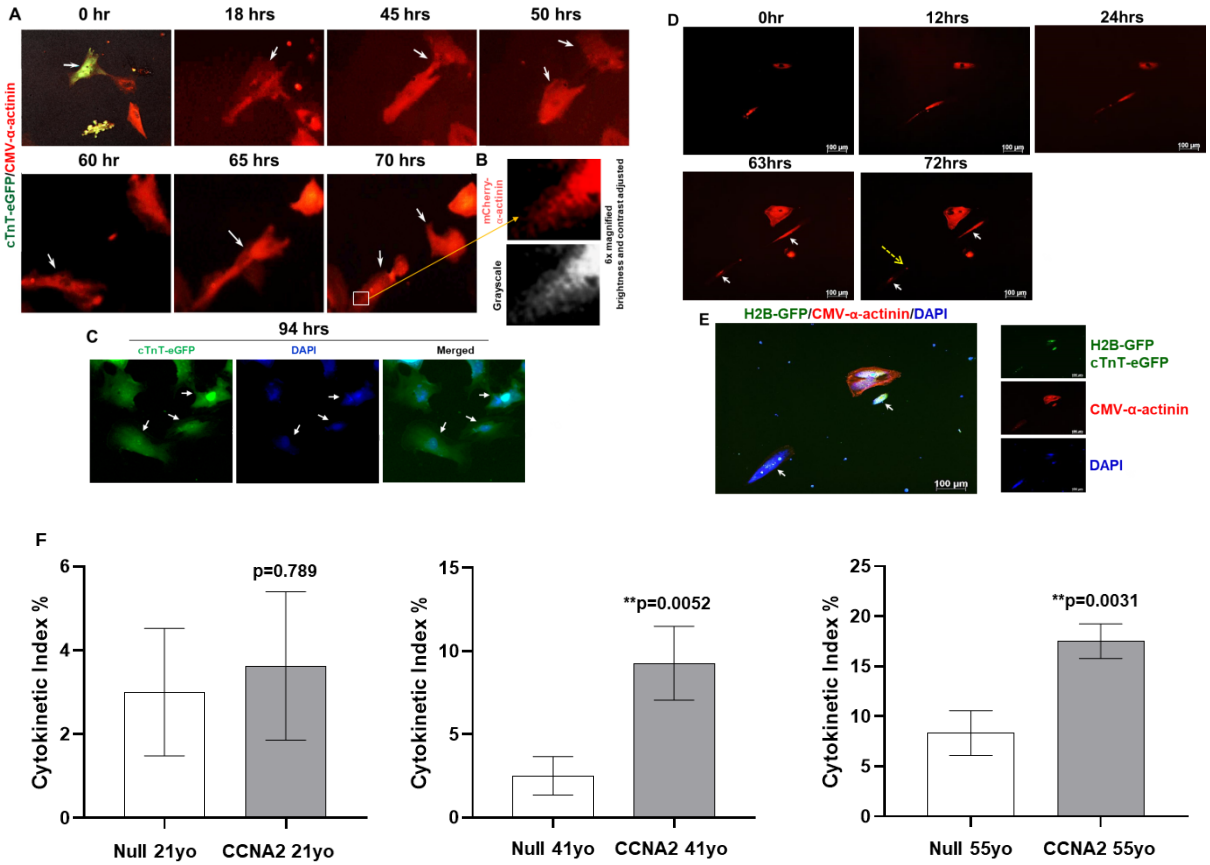

Figure 2: CCNA2 expression induces cytokinesis in adult human cardiomyocytes *In Vitro*. **A, D)** Still images from representative time-lapse epifluorescence microscopy of cultured cardiomyocytes isolated from adult humans (**A**. 55-, **E**. 41-year old). Cells were transfected with cTnT-hCCNA2, cTnT-H2B-GFP, cTnT-eGFP (to label cardiomyocytes), and CMV-α-actinin-m-Cherry adenoviruses prior to the beginning of the time-lapse imaging. At time 0 hr, a cell (yellow) expressing both Troponin Tc (green) and α-actinin (red) was followed for 70 hrs via time-lapse microscopy. The green channel was closed, and cells were only followed through the red channel to avoid UV photo-toxicity. The observed human cardiomyocytes show the 1st cell division at 50 hrs of imaging, and one of the daughter cells subsequently undergoes division at 70 hrs of imaging. **B)** At 70 hrs, a daughter cell is partially magnified with a grayscale version to demonstrate the presence of an intact sarcomere structure. **C, E)** One day after live imaging ended, these wells were fixed with subsequent labeling of nuclei with DAPI. The green fluorescence of the original cTnT-eGFP and cTnT-H2B-GFP transfection are visible, further confirming that these cells are cardiomyocytes. **F)** The cytokinetic events were counted in the control and test samples from the 21-, 41- and 55-year-old subjects. A significantly higher rate of cytokinesis was observed in the test samples from the 41 yo (2.5 ± 1.16 vs. 9.27 ± 2.22, p=0.005) and 51 yo (8.33 ± 2.25 vs. 17.52 ± 1.72, *p*=0.003) compared to the control. The control and test samples from the 21-year-old, on the other hand, did not exhibit a significant difference in the cytokinetic events (3.63 ± 1.77 vs 3.00 ± 1.52, *p*=0.789).

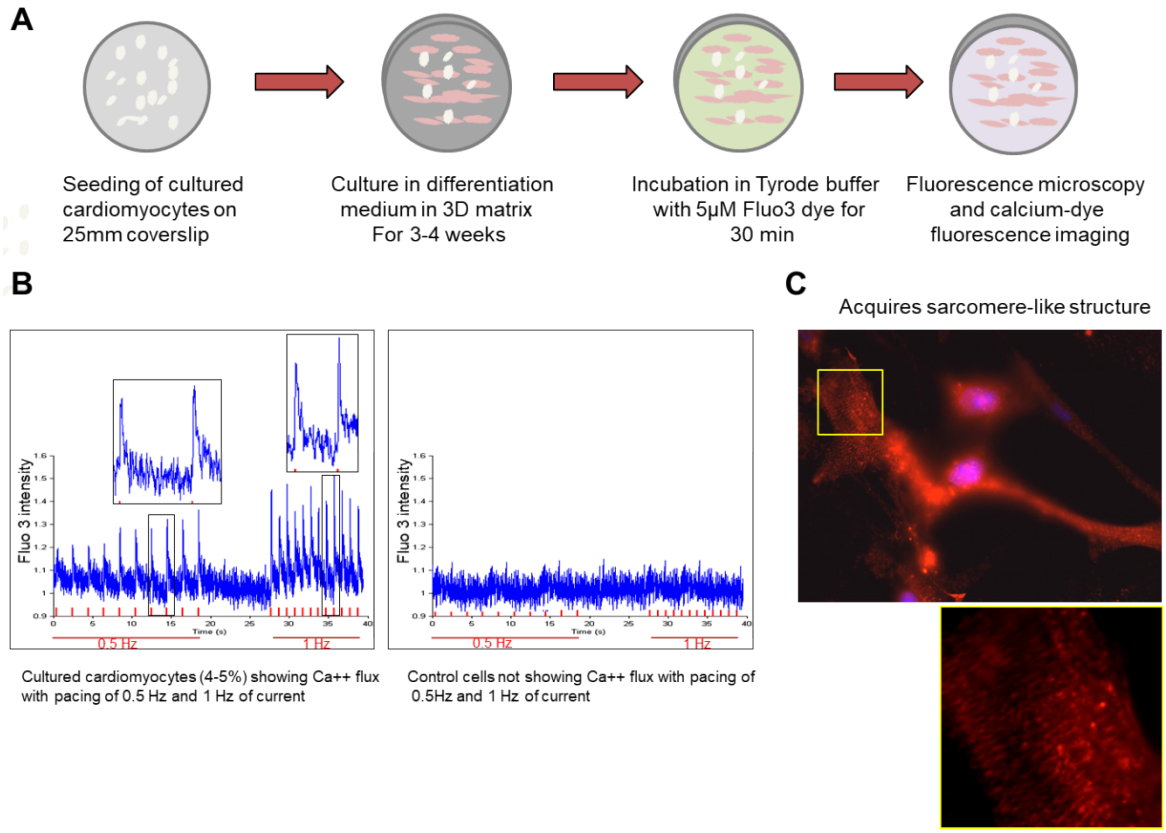

Figure 3: Differentiation of cultured adult human cardiomyocytes. Cultured adult human cardiomyocytes typically undergo dedifferentiation and then were subjected to 3D differentiation culture conditions and examined for calcium flux and re-appearance of the sarcomeric structure. **A)** Overview of the 3D culture method of differentiation, calcium flux measurement and fluorescence microscopy in adult human cardiomyocytes. **B)** Representative calcium flux graphs of re-differentiated cultured adult human cardiomyocytes. Approximately 4-5% of Ad5-cTnT-hCCNA2 transfected adult human cardiomyocytes show Ca++ flux with pacing of 0.5 and 1 Hz of current, while no calcium flux was detected in the non-Ad5-cTnT-hCCNA2 transfected cardiomyocytes. **C)** A representative cardiomyocyte image after re-differentiation. A randomly selected region of the imaged cardiomyocytes is magnified to demonstrate the presence of intact sarcomere structure after re-differentiation in 3D culture.

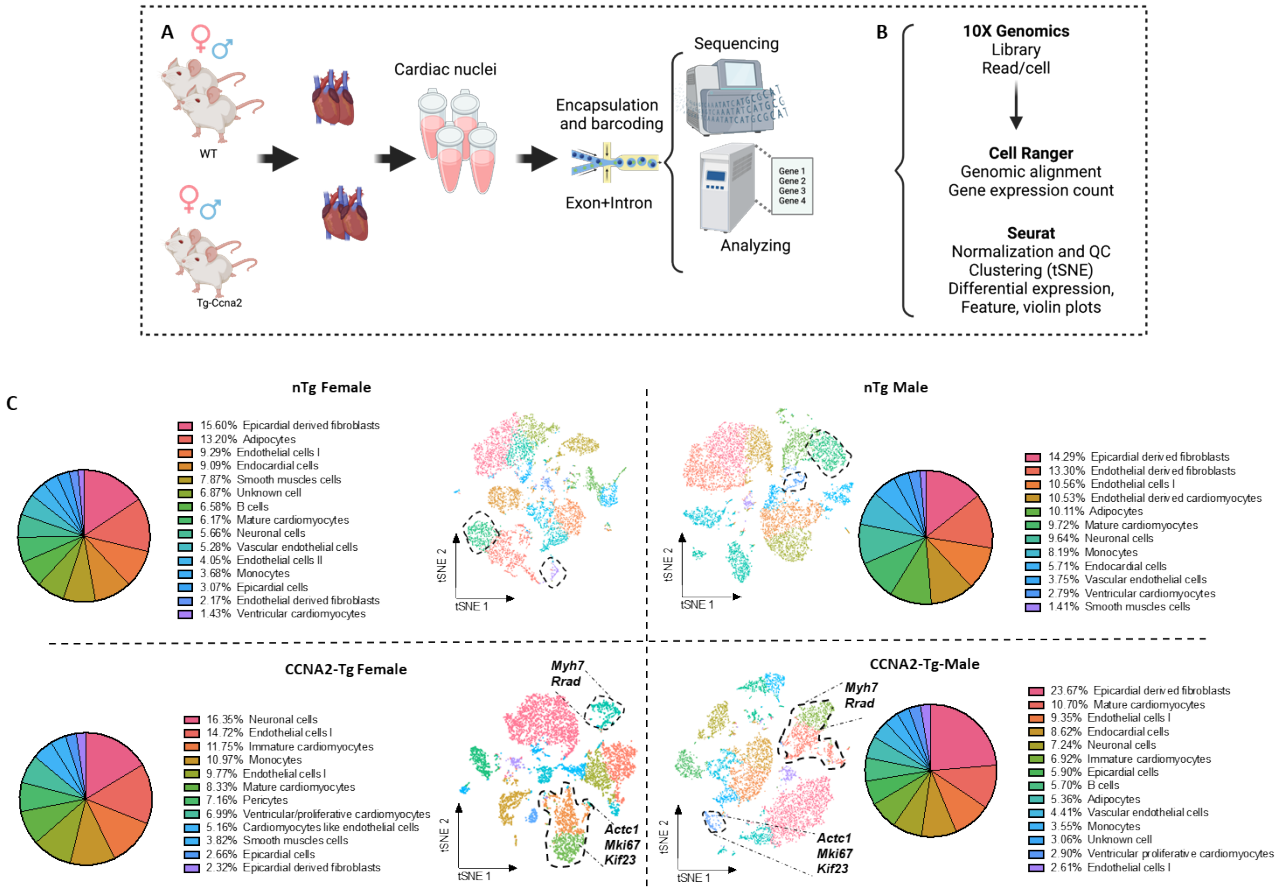

Figure 4: **Single nucleus RNA sequencing identified major cell-types in CCNA2-Tg mice**
A) Schematic depicting the design of the snRNA-seq experiments (n=2) for each condition nTg female, CCNA2-Tg female, nTg male, and nTg male. **B)** The analysis pipeline and single-cell barcoded library generation (10X Genomics), sequence alignment (Cell Ranger), and further analysis using R (SeuratR package). **C)** t-distributed Stochastic Neighbor Embedding (tSNE) clustering the nuclei and reveals more than 14 distinct cell types identified based on the cell-specific markers dataset provided at iRhythmics FairdomHub instance and the pie chart showing the proportion of cells within the snRNA-seq. CMs: Cardiomyocytes**.**

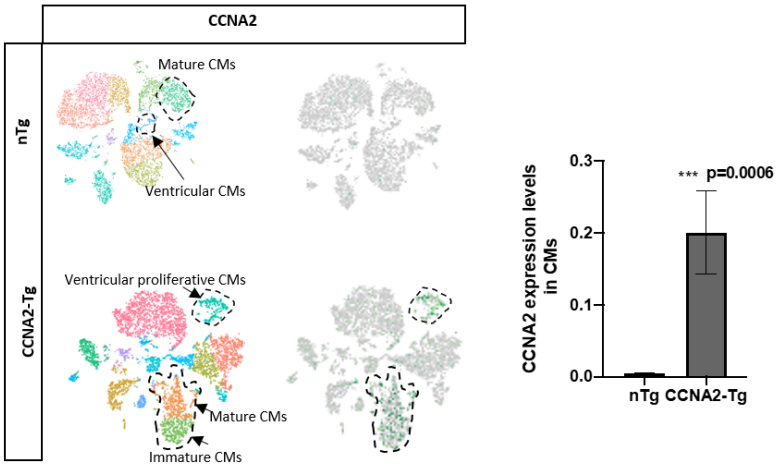

Figure 5: CCNA2 expression in cardiomyocytes of CCNA2-Tg and non-Tg mice delineated by snRNA-seq. A) CCNA2 expressed in a new subset of the cardiomyocyte population in both CCNA2-Tg projected on the t-distributed Stochastic Neighbor Embedding (tSNE) plot. **B)** Representative bar graph showing CCNA2 expression level in cardiomyocytes of CCNA2-Tg and non-Tg mice.

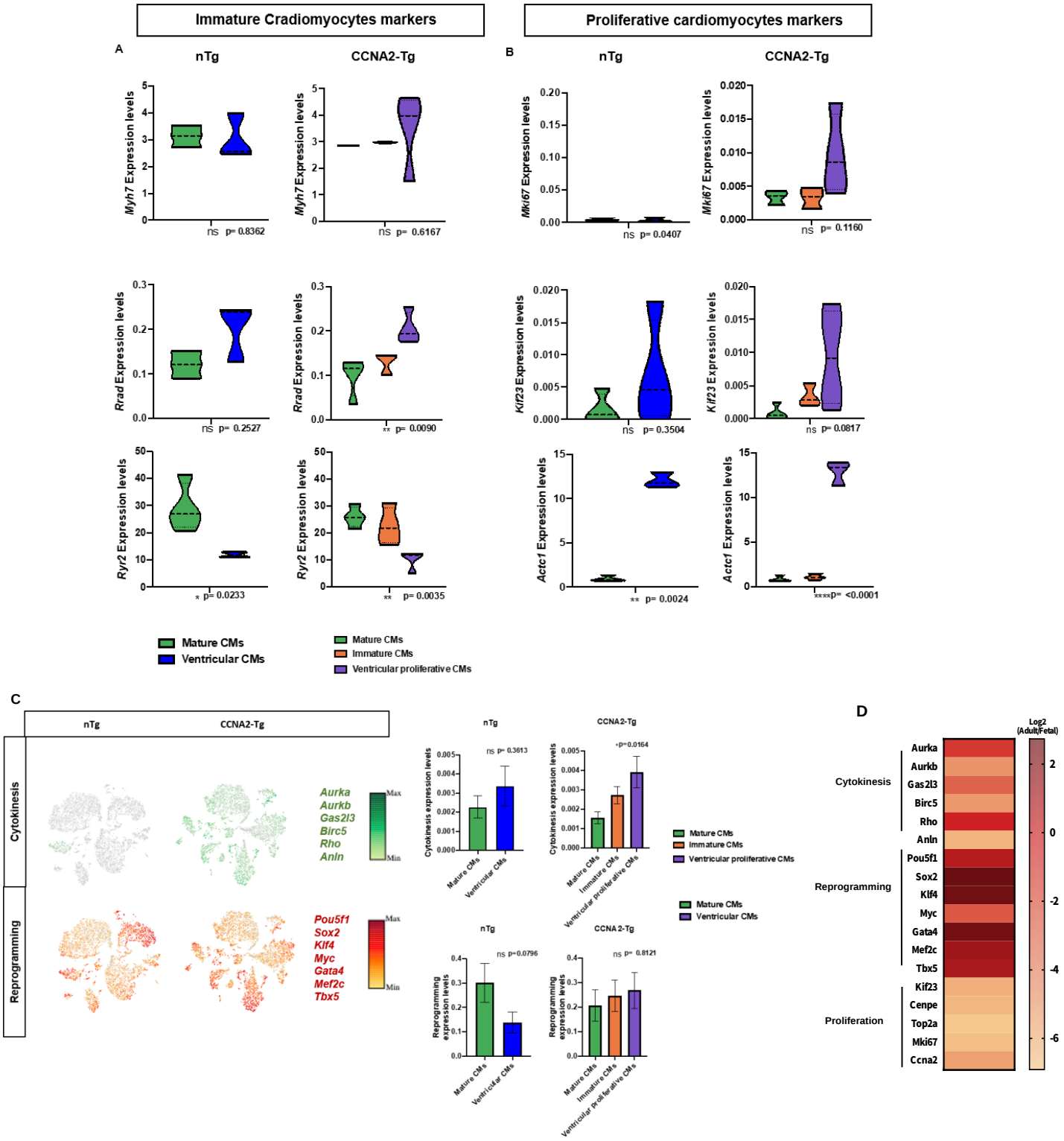

Figure 6: CCNA2 induces new immature and proliferative cardiomyocytes. A) Violin plot representing the expression of immature and proliferative cardiomyocytes markers in both CCNA2-Tg and non-Tg mice. **B)** Representative bar graph showing CCNA2 expression level in cardiomyocytes of CCNA2-Tg and non-Tg mice. **C)** Cytokinesis and reprogramming gene expression projected on tSNE and representative bars of their expression level in cardiomyocytes of CCNA-Tg and non-Tg mice. **D)** Heatmap showing the cytokinesis, reprogramming, proliferation, and cell cycle of log2 adult/fetal human heart.

Figure Legends

Movie (attached): The real-time, live-imaging movie of human adult cardiomyocytes (55-year-old male) is described in **Figure 2**.

Supplementary figure

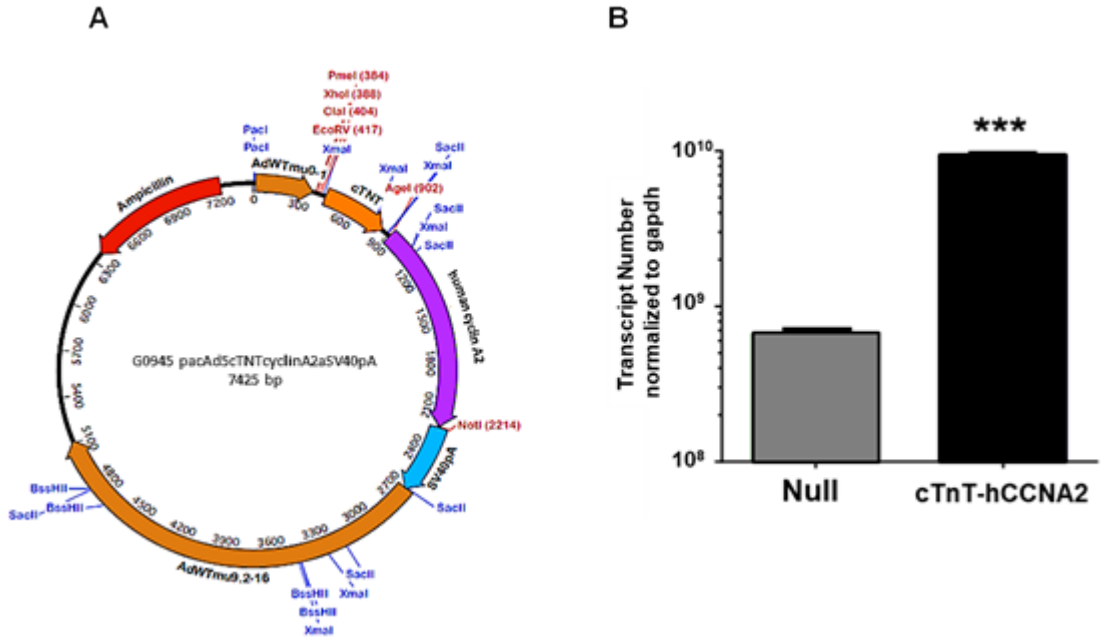

Figure S1: Adenovirus vector construct and CCNA2 expression in adult human cardiomyocytes In Vitro. A) Clinical-use grade replication-deficient human adenovirus type 5 (Ad5) was used for this study. The vector was designed with cardiac Troponin T (cTnT) promoter to express human cyclin A2 (hCCNA2) specifically in cardiomyocytes. B) The cTnT-hCCNA2 adenovirus was used to transfect cultured adult human cardiomyocytes to induce expression of CCNA2. Significantly higher CCNA2 expression was observed in cells transfected with cTnT-hCCNA2 compared to control virus.

Table S1: Table of raw data of cytokinesis events in regions of interest (ROIs) for experimental and control wells.

Table S1

Test (cTNT-CCNA2+cTNT-eGFP)				Control (cTNT-eGFP only)			
ROI	Number of cells	Cytokinetic events	(%)	ROI	Number of cells	Cytokinetic events	(%)
ROI 1	23	5	21.7	ROI 29	13	1	7.7
ROI 2	7	1	14.3	ROI 30	33	1	3.0
ROI 3	17	4	23.5	ROI 31	21	1	4.8
ROI 4	24	7	29.2	ROI 32	9	3	33.3
ROI 5	12	5	41.7	ROI 33	27	3	11.1
ROI 6	11	2	18.2	ROI 34	33	1	3.0
ROI 7	20	4	20.0	ROI 35	29	0	0.0
ROI 8	44	17	38.6	ROI 36	20	1	5.0
ROI 9	26	7	26.9	ROI 37	16	0	0.0
ROI 10	30	6	20.0	ROI 38	30	5	16.7
ROI 11	29	8	27.6	ROI 39	28	1	3.6
ROI 12	32	10	31.3	ROI 40	16	0	0.0
ROI 13	37	6	16.2	ROI 41	17	2	11.8
ROI 14	26	6	23.1	ROI 42	16	2	12.5
ROI 15	18	1	5.6				
ROI 16	47	2	4.3				
ROI 17	40	1	2.5				
ROI 18	19	3	15.8				

ROI 19	18	2	11.1				
ROI 20	20	2	10.0				
ROI 21	22	2	9.1				
ROI 22	34	7	20.6				
ROI 23	27	3	11.1				
ROI 24	21	2	9.5				
ROI 25	9	1	11.1				
ROI 26	14	2	14.3				
ROI 27	15	2	13.3				
ROI 28	23	2	8.7				
		Average	17.8			Average	8.0